



HHS Public Access

Author manuscript

Nat Chem Biol. Author manuscript; available in PMC 2013 July 01.

Published in final edited form as:

Nat Chem Biol. 2013 January ; 9(1): 30–36. doi:10.1038/nchembio.1114.

Identification of DES1 as a Vitamin A Isomerase in Müller Glial Cells of the Retina

Joanna J. Kaylor¹, Quan Yuan¹, Jeremy Cook¹, Shanta Sarfare¹, Jacob Makshanoff¹, Anh Miu¹, Anita Kim¹, Paul Kim¹, Samer Habib¹, C. Nathaniel Roybal¹, Tongzhou Xu¹, Steven Nusinowitz¹, and Gabriel H. Travis^{1,2,*}

¹Jules Stein Eye Institute, University of California, Los Angeles School of Medicine, Los Angeles, CA 90095, USA

²Department of Biological Chemistry, University of California, Los Angeles School of Medicine, Los Angeles, CA 90095, USA

Abstract

Absorption of a light particle by an opsin-pigment causes photoisomerization of its retinaldehyde chromophore. Restoration of light sensitivity to the resulting apo-opsin requires chemical re-isomerization of the photobleached chromophore. This is carried out by a multistep enzyme pathway called the visual cycle. Accumulating evidence suggests the existence of an alternate visual cycle for regenerating opsins in daylight. Here, we identified dihydroceramide desaturase-1 (DES1) as a retinol isomerase and an excellent candidate for isomerase-2 in this alternate pathway. DES1 is expressed in retinal Müller cells where it co-immunoprecipitates with cellular retinaldehyde binding protein (CRALBP). Adenoviral gene therapy with DES1 partially rescued the biochemical and physiological phenotypes in *rpe65*^{-/-} mice lacking isomerohydrolase (isomerase-1). Knockdown of DES1 expression by RNA-interference concordantly reduced isomerase-2 activity in cultured Müller cells. Purified DES1 possessed very high isomerase-2 activity in the presence of appropriate cofactors, suggesting that DES1 by itself is sufficient for isomerase activity.

The first step in visual perception is absorption of a photon by an opsin pigment in the membranous outer segment (OS) of a rod or cone cell. The major chromophore for the vertebrate opsins is 11-*cis*-retinaldehyde (11-*cis*-RAL). Another is 9-*cis*-retinaldehyde (9-*cis*-RAL), which forms iso-opsin pigments of ~50% lower quantum efficiency¹. 9,13-di-*cis*-retinaldehyde (9,13-di-*cis*-RAL) forms iso-opsin II pigments of similar quantum efficiency to iso-opsin pigments¹. Photon capture by an opsin pigment causes isomerization of its 11-*cis*-RAL or 9-*cis*-RAL to all-*trans*-retinaldehyde (all-*trans*-RAL). The resulting

Users may view, print, copy, download and text and data- mine the content in such documents, for the purposes of academic research, subject always to the full Conditions of use: http://www.nature.com/authors/editorial_policies/license.html#terms

*Corresponding author: travis@jsei.ucla.edu.

Author contributions

G.H.T. conceived the project. G.H.T., J.J.K., C.N.R., Q.Y., and S.N. designed the experiments and interpreted the data. J.J.K., Q.Y., J.C., S.S., J.M., A.M., A.K., P.K., S.H., T.X., and C.N.R. performed the experiments. G.H.T. wrote the manuscript.

Competing Financial Interests

The authors declare no competing financial interests.

metarhodopsin II briefly activates the visual-transduction cascade before decaying to yield free all-*trans*-RAL and apo-opsin. Following its release from bleached opsin, all-*trans*-RAL is converted back to 11-*cis*-RAL by a multi-step enzyme pathway in RPE cells called the visual cycle (Fig. 1). The critical re-isomerization step is catalyzed by Rpe65 (isomerohydrolase or isomerase-1), which converts an all-*trans*-retinyl ester (all-*trans*-RE) such as all-*trans*-retinyl palmitate (all-*trans*-RP) to 11-*cis*-retinol (11-*cis*-ROL)^{2,3}. The final product of the RPE visual cycle is 11-*cis*-RAL, which is released into the interphotoreceptor matrix (IPM) where it binds interphotoreceptor-retinoid binding protein (IRBP). The 11-*cis*-RAL is subsequently taken up by the photoreceptor where it recombines irreversibly with apo-opsin to form a new light-sensitive pigment.

Several observations suggest the existence of a second pathway for visual-chromophore regeneration in Müller glial cells of the retina. For example, regeneration of photobleached rod and cone opsins was observed in retinas separated from the RPE^{4,5}. Isolated salamander and mouse cones, but not rods, regained sensitivity following light exposure upon addition of 11-*cis*-ROL, while both rods and cones regained sensitivity upon addition of 11-*cis*-RAL⁶⁻⁸. The source of this 11-*cis*-ROL appears to be retinal Müller cells. For example, cultured Müller cells were shown to take-up all-*trans*-ROL and isomerize it to 11-*cis*-ROL, which they secreted into the medium⁹. Müller cells were shown to be responsible for the regeneration of bleached photopigments in retinas separated from the RPE^{7,8}. Finally, Müller cells express multiple proteins involved in the processing of visual retinoids including cellular retinaldehyde binding protein (CRALBP)¹⁰, cellular retinol binding protein (CRBP)¹¹, and retinol dehydrogenase type-10 (RDH10)¹². The maximum rate of 11-*cis*-ROL-synthesis by Rpe65 is slower than the estimated rate of visual-pigment photoisomerization in the eye under daylight conditions¹³, implying the need for another mechanism to generate chromophore. A second retinol isomerase activity was shown to be present in crude homogenates of cone-dominant retinas from chickens and ground-squirrels¹³⁻¹⁵. Unlike Rpe65, which uses an all-*trans*-RE as substrate^{2,3,16}, isomerase-2 in retinas acts directly on all-*trans*-ROL^{13,14}. In the current work, we identified the protein responsible for this isomerase-2 activity.

RESULTS

Identification of Isomerase-2 by Expression Screening

To identify isomerase-2, we performed a high-throughput expression screen using an abundance-normalized cDNA library from chicken neural-retinas. We separated the library into 100 pools of ~800 clones per pool and transfected plasmid from each pool into HEK-293T (293T) cells. Then, we screened homogenates from each dish of cells for isomerase-2 activity using an assay system previously used to show isomerase-2 activity in chicken and ground-squirrel retina homogenates^{13,14}. A representative chromatogram showing separation of the retinol isomers is presented in Supplementary Results, Supplementary Fig. 1. UV spectra for all retinol isomers are shown in Supplementary Fig. 1b-f). Isomerase-2 activities in homogenates of 293T cells transfected with the parent pool, subpool, and candidate isomerase-2 clone (#15.36.21) from the chicken retina library are shown in Supplementary Fig. 2.

Sequence analysis of clone #15.36.21 showed it to encode dihydroceramide 4-desaturase-1 (DES1) (NM_001012565.1)¹⁷. DES1 introduces a 4,5-*trans*-double bond in dihydroceramide as the final step in ceramide synthesis^{17,18}, and is a member of the membrane desaturase family. These proteins contain three conserved histidine motifs: HX₍₃₋₄₎H ... HX₍₂₋₃₎HH ... HX₍₂₋₃₎HH that define two oxo-bridged diiron binding clusters¹⁹. DES1 is an endoplasmic reticulum (ER) protein with four transmembrane segments^{19,20}. It is also *N*-myristoylated²¹, which targets DES1 to mitochondria²². DES1 is coupled to the cytochrome *b*₅ electron-transport chain, and acts via a free-radical mechanism²⁰.

DES1 is Expressed in Müller Glial Cells

DES1 is expressed in multiple tissues including brain, liver, kidney, and skin²³. To determine its distribution within the retina, we performed immunohistochemistry on mouse retina sections using an antibody against mouse DES1. Similar to CRALBP¹⁰, DES1 was located in Müller cells (Fig. 2A). Interestingly, both DES1 and CRALBP were expressed in Müller-cell apical process, which extend into the IPM beyond the outer-limiting membrane (Fig. 2A). The IPM also contains rod and cone OS, and hence is the likely region of retinoid exchange between photoreceptors and Müller cells. Both DES1 and CRALBP were also present in the Müller-cell endfeet within the ganglion cell layer (GCL) (Fig. 2a). Immunoblot analysis showed that DES1 was present at similar levels in retina and RPE (Fig. 2b and Supplementary Fig. 3). DES1 appeared as a doublet band due to the presence of myristoylated and non-myristoylated forms²⁴. DES1 was also abundantly expressed in primary cultured chicken Müller cells (Fig. 2b and Supplementary Fig. 3).

Inhibitors of DES1 Isomerase-2 Activity

If dihydroceramide and retinol are both substrates for DES1, dihydroceramide may inhibit DES1-catalyzed retinol isomerization. Accordingly, we assayed isomerase-2 activity in the presence of increasing dihydroceramide concentrations. Homogenates of 293T-D cells, which stably express chicken DES1, were used as an enzyme source. We also performed this experiment in the presence of cyclopropenylceramide, a non-desaturable analog that competitively inhibits DES1-catalyzed ceramide synthesis²⁵. Both agents inhibited isomerase-2 activity (Supplementary Fig. 4a).

Another competitive inhibitor of the dihydroceramide desaturase reaction is *N*-(4-hydroxyphenyl)-retinamide (fenretinide or 4-HPR) with a $K_i = 8.3 \mu\text{M}$ ²⁶. Fenretinide is structurally similar to all-*trans*-ROL (Supplementary Fig. 4b). We assayed homogenates of DES1-transfected 293T cells for isomerase-2 activity at various concentrations of all-*trans*-ROL and fenretinide. Lineweaver-Burke transformation of these data showed that fenretinide is a competitive inhibitor of DES1-catalyzed isomerase-2 activity with a $K_i = 8.5 \mu\text{M}$ (Supplementary Figs. 4c and d). Together, the results of these inhibitor experiments establish a link between the dihydroceramide desaturase and isomerase-2 activities of DES1.

Isomerase-2 Activities of Other Membrane Desaturases

DES1 is a member of the membrane-desaturase family. To determine whether retinol-isomerase activity is a general property of these metalloproteins, or one unique to DES1, we

subcloned cDNA's for the human membrane-desaturases: DES1, DES2, FADS1, FADS2, and SCD into a eukaryotic expression-plasmid. DES1 and DES2 are 64% identical, while the other desaturases exhibit lower levels of identity with DES1. We transfected the membrane-desaturase plasmids into 293T cells and assayed cell homogenates for isomerase-2 activity using all-*trans*-ROL as substrate. The rate of 11-*cis*-ROL synthesis was dramatically higher for DES1 versus the other membrane desaturases (Figs. 3a). Thus, retinol-isomerase activity is a unique feature of DES1, and not a general property of membrane desaturases or diiron-binding proteins.

DES1 Catalyzes Equilibrium Isomerization of Retinol

The data presented in Figs. 3a–d illustrate another property of DES1-catalyzed retinol isomerization. The ratios of (11-*cis*-ROL):(9,13-di-*cis*-ROL):(9-*cis*-ROL):(13-*cis*-ROL) synthesized from all-*trans*-ROL by DES1 were (1):(78):(158):(388). These ratios are similar to the published equilibrium ratios of (1):(40):(109):(231) for the same retinoid isomers following incubation of all-*trans*-RP with I₂ catalyst²⁷. These data suggest that DES1 catalyzes the equilibrium isomerization of retinol. In an equilibrium mixture, the abundance of each species varies inversely with its free energy. Of the retinol isomers, sterically strained 11-*cis*-ROL has the highest free energy while planar all-*trans*-ROL has the lowest, with an energy difference between them of 4.1 kcal/mol²⁸.

We measured the substrate kinetics of chicken DES1-catalyzed retinol isomerization using all-*trans*-ROL and 11-*cis*-ROL substrates (Supplementary Figs. 5a–h). These data yielded K_M and V_{max} values for each reaction. From all-*trans*-ROL substrate, the V_{max} was 4.3 pmol/min/mg for synthesis of 11-*cis*-ROL, 46 pmol/min/mg for synthesis of 9,13-di-*cis*-ROL, 65 pmol/min/mg for synthesis of 9-*cis*-ROL, and 1730 pmol/min/mg for synthesis of 13-*cis*-ROL (Supplementary Fig. 5a–d). Hence, the rates of all-*trans*-ROL conversion to its *cis*-isomers varied inversely with the free-energy change of each reaction. In the thermodynamically favored 'reverse' direction V_{max} values were higher, with a net conversion rate of 11-*cis*-ROL to 9-*cis*-ROL, 13-*cis*-ROL and all-*trans*-ROL of 2,950 pmol/min/mg (Supplementary Figs. 5e–h). These kinetic data provide further evidence that DES1 catalyzes the equilibrium isomerization of retinols. The K_M values for the DES1-catalyzed reactions were all within the range of 15–21 μ M except for all-*trans*-ROL-dependent synthesis of 9,13-di-*cis*-ROL and 9-*cis*-ROL, where the K_M 's were 4.3 and 7.7 μ M, suggesting that DES1 is a more efficient catalyst for synthesis of 9,13-di-*cis*-ROL and 9-*cis*-ROL at low all-*trans*-ROL concentrations.

DES1 Expression in Rod- and Cone-dominant Retinas

Isomerase-2 activity was much lower in retina homogenates from rod-dominant mice and cattle versus cone-dominant chickens and ground squirrels^{13,14}. A possible explanation is lower catalytic efficiency of DES1 orthologs from rod- versus cone-dominant species. Alternatively, DES1 may be expressed at lower levels in rod- versus cone-dominant retinas, with similar catalytic efficiencies. To discriminate between these possibilities, we measured DES1 mRNA levels in chicken, mouse and cow retinas by qRT-PCR. The DES1 mRNA level was five-fold higher in chicken versus mouse or cow retinas (Supplementary Fig. 6a). In contrast, we observed similar isomerase-2 specific activities in homogenates of 293T cells

transfected with plasmids for chicken, mouse or human DES1 (Supplementary Fig. 6b). Thus, the greater isomerase-2 activities observed in the cone-dominant species is due to higher expression of DES1.

DES1 (Fig. 3d) and Rpe65²⁹ synthesize 13-*cis*-ROL from all-*trans*-ROL and all-*trans*-RP, respectively. However, DES1 is the only known source of 9-*cis*-retinoids in vertebrates. If DES1 is responsible for isomerase-2 activity, we would expect higher levels of 9-*cis*- and 13-*cis*-retinoids in chicken versus mouse retinas. To test this prediction, we measured levels of endogenous retinoids from dark-adapted mouse and chicken retinas, normalized to total protein (Table 1). Levels of 11-*cis*-RAL were similar in chicken and mouse retinas. In contrast, 9-*cis*-RAL was 26-fold more abundant in dark-adapted chicken versus mouse retinas. Thus, 9-*cis*-RAL comprised nearly 7% of visual chromophore in chickens, but only 0.2% of chromophore in mice. 13-*cis*-RAL was also much higher in chicken versus mouse retinas (Table 1). The higher levels of 9-*cis*-RAL and 13-*cis*-RAL probably reflect the greater expression of DES1 in chicken versus mouse retinas (Supplementary Fig. 5a). Despite dark-adaptation for four hours, chicken retinas contained significant all-*trans*-RAL (Table 1), as was previously reported³⁰. In contrast to rhodopsin, cone-opsins dissociate to yield apo-opsin and free chromophore³¹. Since retinols and retinaldehydes freely interconvert through the action of multiple retinol dehydrogenases, the persistence of all-*trans*-RAL in dark-adapted chicken retinas may reflect the high isomerase-2 activity in these retinas^{13,14}.

Gene Therapy of *rpe65*^{-/-} mice with ad-DES1

An argument against the existence of a second retinoid isomerase is that retinas from *rpe65*^{-/-} mice with a null mutation in the gene for isomerase-1 contain virtually no 11-*cis*-RAL³². If a second isomerase were present in retinas, it should partially complement the *rpe65*^{-/-} phenotype. To explore this incongruity, we measured DES1 expression in three-month-old wild-type (129/Sv) and *rpe65*^{-/-} retinas. Levels of the *des1* mRNA were 6.6-fold lower in *rpe65*^{-/-} versus wild-type retinas by qRT-PCR (Supplementary Fig. 6c). Comparably reduced levels of DES1 protein were also observed in three-month-old *rpe65*^{-/-} versus wild-type retinas by immunoblotting (Supplementary Fig. 6d). At one month, *des1* mRNA levels were only reduced by ~30% in *rpe65*^{-/-} versus wild-type mouse eyes by qRT-PCR normalized to 18S rRNA, suggesting that the loss of DES1 expression is coupled to cone degeneration in *rpe65*^{-/-} mice³³. The more severe than expected phenotype in *rpe65*^{-/-} mice may be caused by very low DES1 expression. To test this possibility, we prepared recombinant adenoviruses containing a CMV promoter upstream of the coding region for human DES1 (ad-DES1) or red-fluorescent protein (ad-RFP). We injected ad-DES1 or ad-RFP intravitreally into *rpe65*^{-/-} mice. Injection into the vitreal space targets Müller cells, whose endfeet contact the vitreal surface. Further, the ad5-serotype has tropism for Müller cells³⁴. Hence, Müller cells were likely targets for adenoviral transduction. Other cells in the inner retina also may have been transduced. Total *DES1* mRNA levels (mouse plus human) increased approximately two-fold after 24 hours in ad-DES1- versus ad-RFP-injected *rpe65*^{-/-} mice by qRT-PCR normalized to 18S rRNA. We measured visual retinoids in *rpe65*^{-/-} retinas one day after injection of ad-DES1 or ad-RFP. Levels of 9-*cis*-RAL were three-fold higher in mice that received ad-DES1 (Fig. 4a).

However, 11-*cis*-retinoids were undetectable in these mice. This may be due to the low levels of all-*trans*-ROL in *rpe65*^{-/-} retinas and the lower K_M for conversion of all-*trans*-ROL to 9-*cis*-ROL versus 11-*cis*-ROL (Supplementary Fig. 5b). Accordingly, we injected all-*trans*-ROL into the vitreal space of *rpe65*^{-/-} mice 18 hours after ad-DES1 or ad-RFP injection. In retinas from these vitamin A-supplemented eyes, both 11-*cis*-RAL and 9-*cis*-RAL increased in ad-DES1 versus ad-RFP injected mice (Fig. 4b).

To test for rescue of visual function, we performed electroretinography (ERG) in *rpe65*^{-/-} mice, where one eye was injected with ad-DES1 and the other with ad-RFP. Representative raw ERG tracings are shown in Fig. 4c. The responses were recorded to light flashes modulated at 10-Hz under dark-adapted conditions. For the representative tracings, response amplitudes were approximately three-fold higher in the *rpe65*^{-/-} eye that received ad-DES1 versus ad-RFP. A Fourier transformation was performed on each of the raw waveforms to extract the signal yoked to the stimulus presentation frequency of 10-Hz. The difference in Fourier-derived ERG amplitudes between ad-DES1- versus ad-RFP-injected eyes are shown (Fig. 4d). Data points above the zero line indicate that the ad-DES1 injected eye performed better than the ad-RFP-injected eye. At every flash intensity, *rpe65*^{-/-} eyes that received ad-DES1 showed higher amplitudes than ad-RFP-injected eyes. Thus, increasing expression of DES1 several-fold above the low levels in *rpe65*^{-/-} eyes commensurately increased levels of visual chromophore and functional photosensitivity in these mutant mice. Partial rescue of the biochemical and physiological phenotype in *rpe65*^{-/-} mice by adenoviral gene-therapy suggests that DES1 also functions as a retinol isomerase *in vivo*.

Co-immunoprecipitation of CRALBP with DES1

CRALBP binds 11-*cis*- and 9-*cis*-RAL's and 11-*cis*-ROL with nanomolar affinities, but has low affinity for 13-*cis*- and all-*trans*-retinoids^{35,36}. CRALBP may therefore play a role in driving DES1-catalyzed isomerization of all-*trans*-ROL to 11-*cis*-ROL. To check for a direct interaction between these proteins, we attempted to co-immunoprecipitate CRALBP with DES1. Homogenates of chicken retinas were incubated with immobilized, affinity-purified antibodies against chicken DES1. After washing, we eluted the bound proteins and analyzed all fractions by immunoblotting. Both DES1 and CRALBP were present in the eluate (Fig. 5a and Supplementary Fig. 7). To test for non-specific binding of CRALBP to immobilized DES1 antibodies, we loaded homogenates of 293T cells expressing CRALBP onto the same column and analyzed for CRALBP immunoreactivity in the eluate. None was detectable (Fig. 5a), ruling-out non-specific interactions between CRALBP and immobilized DES1 antibodies. Next, we tested for reciprocal immunoprecipitation of DES1 by CRALBP using a column containing immobilized CRALBP antibodies. We observed no DES1 immunoreactivity in the eluate (Fig. 5a), possibly due to epitope-masking or because CRALBP is much more abundant than DES1 in chicken retinas (Fig. 5a). Finally, we tested for co-immunoprecipitation of DES1 with Müller-cell ER protein, RDH10¹². In contrast to CRALBP, RDH10 did not co-immunoprecipitate with DES1. Co-immunoprecipitation of CRALBP by DES1 suggests a direct interaction between these proteins.

To test for an effect of CRALBP on isomerase-2 activity, we transiently transfected 293T-D cells, which stably express DES1, with a plasmid containing chicken-CRALBP or with non-

recombinant pcDNA. We quantified the retinol *cis*-isomers synthesized from all-*trans*-ROL by these cell homogenates. Synthesis of 11-*cis*-ROL increased three-fold and 9-*cis*-ROL 1.4-fold in the presence of CRALBP (Fig. 5b). In contrast, the presence of CRALBP reduced synthesis of 13-*cis*-ROL (Fig. 5b). These data show that CRALBP augments synthesis of chromophore-precursors by DES1.

RNAi Knockdown of DES1 expression in Müller cells

To corroborate our identification of isomerase-2, we attempted to knockdown its catalytic activity using RNA-interference (RNAi) in primary cultured chicken Müller cells with a small-interfering RNA (siRNA) against DES1. Cells transfected with the DES1-siRNA showed an approximate 50% reduction in DES1 mRNA by qRT-PCR (Supplementary Fig. 8a). Similarly, the DES1 protein was reduced approximately 50% in Müller cells treated with the DES1-siRNA by quantitative immunoblotting (Supplementary Fig. 8b). We analyzed homogenates of both cells for isomerase-2 activity using all-*trans*-ROL or 11-*cis*-ROL substrates. In the forward direction, we observed 50–60% lower rates of 11-*cis*-ROL, 9,13-di-*cis*-ROL, 9-*cis*-ROL and 13-*cis*-ROL synthesis by homogenates of cells transfected with the DES1-siRNA versus a non-silencing (ns) control RNA (Supplementary Fig. 8c). Consumption of all-*trans*-ROL substrate was also reduced in reactions containing siRNA-versus ns-RNA-transfected homogenates (Supplementary Fig. 8b). A similar pattern was observed when the isomerase reactions were carried out in the reverse direction. The rates of 9-*cis*-ROL, 13-*cis*-ROL and all-*trans*-ROL synthesis from 11-*cis*-ROL by homogenates of Müller cells transfected with DES1-siRNA were 50–65% lower than by ns-RNA-transfected cell homogenates (Supplementary Fig. 8d). Thus, the decrease in DES1 expression and reduction of isomerase-2 activity were concordant.

Purified DES1 Has Isomerase-2 Activity

The data presented above are consistent with two possibilities: (i) DES1 is isomerase-2, or (ii) DES1 is not isomerase-2 but is required for isomerase-2 activity. To discriminate between these, we expressed chicken DES1 in *E. coli* as an *N*-terminal glutathione *S*-transferase (GST) fusion-protein, and purified GST-DES1 by glutathione affinity-chromatography. Fractions from the column were separated by SDS-PAGE. After extensive washing, the eluate from the glutathione column showed a single band of the expected size on a silver-stained Laemmli gel (Supplementary Fig. 9a). This band exhibited DES1 immunoreactivity by Western blotting (Supplementary Fig. 9b). To rule out isomerase-2 activity by GST fusion-partner, we expressed and affinity-purified GST alone (Supplementary Fig. 9c). We then measured the rates of all-*trans*-ROL conversion to 11-*cis*-ROL, 9,13-di-*cis*-ROL, 9-*cis*-ROL and 13-*cis*-ROL by the different protein fractions. Cytochrome *b*₅, ferredoxin and iron(III) sulfate were added to each assay mixture to compensate for the loss of these components during purification. Purified GST-DES1 exhibited dramatically higher isomerase-2 activities (Supplementary Fig. 9d). For example, the specific activities of isomerase-2 in the GST-DES1 eluate fraction were 100–400-fold higher than those of the preload fraction (Supplementary Fig. 9d), and 20–130-fold higher than the calculated V_{\max} values for homogenates of DES1-transfected 293T cells (Supplementary Figs. 5a–c). GST without DES1 exhibited negligible isomerase-2 activity

(Supplementary Fig. 9d), indicating that the DES1-component of GST-DES1 is responsible for the observed activity.

DISCUSSION

DES1 is a membrane desaturase that introduces a double bond at a non-activated position in an alkyl chain of dihydroceramide^{17,18}. Here, we show that DES1 also catalyzes the equilibrium isomerization of retinol. Addition of all-*trans*-ROL to homogenates of primary cultured chicken Müller cells that express DES1 (Supplementary Fig. 8), DES1-expressing 293T cell-homogenates (Figs. 3 and 5), and purified DES1 expressed in *E. coli* (Supplementary Fig. 9) resulted in formation 11-*cis*-ROL, 9,13-di-*cis*-ROL, 9-*cis*-ROL, and 13-*cis*-ROL at ratios similar to those seen following iodine-catalyzed retinoid equilibration²⁷. The rate of DES1-catalyzed retinoid equilibration was very high. To illustrate, the net V_{\max} for all-*trans*-ROL conversion to its four *cis*-isomers was $\sim 1,850$ pmol/min/mg-protein (Supplementary Figs. 5a–d) by 293T-D cell-homogenates. In contrast, the published V_{\max} for conversion of all-*trans*-RP to 11-*cis*-ROL by bovine Rpe65 was 26 pmol/min/mg-protein² using recombinant-baculovirus infected *Sf9*-cell homogenates². The DES1 protein was at least 10-fold less abundant in 293T-D homogenates than was Rpe65 in the *Sf9* homogenates². Assuming equal ratios of 11-*cis*-ROL and 13-*cis*-ROL synthesized by Rpe65²⁹, the maximum retinoid-isomerase rate of DES1 is at least 300-fold higher than that of Rpe65.

Vertebrate opsins utilize 11-*cis*-RAL and 9-*cis*-RAL as chromophore, but not 13-*cis*-RAL. Given the thermodynamically favored synthesis of 13-*cis*-ROL, what mechanisms might drive synthesis of 11-*cis*-ROL and 9-*cis*-ROL by DES1? A model for the function of DES1 illustrating potential mechanisms of mass action in the context of the vertebrate retina is shown in Fig. 6. Following light exposure, rods and cones release all-*trans*-ROL into the IPM. This all-*trans*-ROL is taken up by Müller cells, where it is subjected to DES1-catalyzed equilibrium-isomerization. CRALBP, which physically associates with DES1 (Fig. 5a), binds 11-*cis*-ROL with nanomolar affinity, but not 13-*cis*-ROL or all-*trans*-ROL^{35,36}. CRALBP was shown to release its retinoid ligand on association with acidic phospholipids of the plasma membrane³⁷, providing a mechanism for the transfer of 11-*cis*-ROL to IRBP in the IPM, and for continuous regeneration of apo-CRALBP. Cones, but not rods, contain an as-yet unidentified NADP⁺-dependent retinol dehydrogenase that oxidizes 11-*cis*-ROL, and probably 9-*cis*-ROL, to their cognate aldehydes¹³. The presence of this dehydrogenase explains the capacity of bleached cones, but not rods, to recover photosensitivity upon addition of 11-*cis*-ROL^{6–8}. Removal of 11-*cis*-ROL and 9-*cis*-ROL by oxidation, and subsequent formation of opsin pigments from the resulting 11-*cis*-RAL and 9-*cis*-RAL, represent two other mechanisms to drive continued synthesis of 9-*cis*-ROL and 11-*cis*-ROL by DES1.

9-*cis*-RAL combines with apo-rhodopsin to form stable, photosensitive iso-rhodopsin³⁸. The role of iso-opsin pigments in cones, however, has not been studied. DES1 preferentially synthesizes 9-*cis*-ROL over 11-*cis*-ROL *in vitro* (Supplementary Figs. 5a and c, 9d). If DES1 functions in the alternate visual cycle as proposed (Fig. 6), cone-dominant retinas should possess a larger fraction of iso-opsin pigments than rod-dominant retinas. Indeed,

chicken retinas contained 26-fold higher 9-*cis*-RAL than did mouse retinas (Table 1). Given that the percentage of cones is 20-fold higher in chicken versus mouse retinas^{39,40}, 9-*cis*-RAL may represent an important alternate chromophore for the cone opsins. Utilization of 9-*cis*-RAL chromophore can also be detected in *rpe65*^{-/-} mice. Although 11-*cis*-retinoids are undetectable, these animals are not blind. At high stimulus intensities, the ERG response in *rpe65*^{-/-} mice approaches 25% of the amplitude in wild-type mice^{41,42}. This light sensitivity is likely mediated by iso-rhodopsin, since *rpe65*^{-/-} retinas contain small amounts of 9-*cis*-RAL (Fig. 4a). With prolonged dark adaptation, *rpe65*^{-/-} mice accumulate significant 9-*cis*-RAL and exhibit rod ERG-responses of up to 40% the amplitude in wild-type mice⁴³. DES1 is the likely source of 9-*cis*-retinoids despite the low abundance of this protein in *rpe65*^{-/-} retinas. Following intravitreal injection of ad-DES1 into *rpe65*^{-/-} eyes, levels of 9-*cis*-RAL increased several-fold (Fig. 4a). No 11-*cis*-RAL was formed, however (Fig. 4a), due to the much lower K_M for all-*trans*-ROL-dependent synthesis of 9-*cis*-ROL versus 11-*cis*-ROL (Supplementary Figs. 5a and b). However, both 9-*cis*-RAL and 11-*cis*-RAL were present in ad-DES1-injected *rpe65*^{-/-} eyes that received supplemental all-*trans*-ROL (Fig. 4b). The increased 9-*cis*-RAL in ad-DES1 injected *rpe65*^{-/-} eyes was accompanied by a several-fold increase in ERG amplitudes (Figs. 4c and d). Müller cells express RDH10, which oxidizes retinol to retinaldehyde with low isomeric specificity^{12,44}. Thus, Müller cells may also provide ‘completed’ 9-*cis*-RAL for use by rods. This would explain the presence of iso-rhodopsin in *rpe65*^{-/-} rods.

Cones gain two important benefits by taking up 9-*cis*-ROL or 11-*cis*-ROL and oxidizing it *in situ* to 9-*cis*-RAL or 11-*cis*-RAL (Fig. 6). The rod response saturates at photoisomerization rates beyond 500 per second⁴⁵. At this point, rods contribute nothing to visual perception. Despite rod saturation, rhodopsin pigments continue to photoisomerize with increasing light. Hence, cones must compete with saturated rods for limiting supplies of chromophore. Cones can escape this competition by taking up 9-*cis*-ROL and 11-*cis*-ROL for ‘in house’ synthesis of chromophore. Thus, the alternate visual cycle in Müller cells represents a ‘private pipeline’ of chromophore precursor for cones. With this pathway in place, rods assist rather than compete with cones by providing all-*trans*-ROL substrate for DES1 in Müller cells. Finally, oxidation of 9-*cis*-ROL or 11-*cis*-ROL and reduction of all-*trans*-RAL occur simultaneously in cones utilizing the alternate visual cycle. Cones thereby gain a locally self-renewing supply of NADPH cofactor (Fig. 6). This eliminates the high energetic burden of synthesizing NADPH cofactor⁴⁶, allowing cones to operate at high sustained rates of photoisomerization.

Both Rpe65²⁹ and DES1 (Fig. 3c) produce 13-*cis*-ROL. Once formed, 13-*cis*-ROL may be oxidized to 13-*cis*-RAL or fatty-acylated to a 13-*cis*-RE. However, vertebrate opsins cannot utilize 13-*cis*-RAL as visual chromophore. No enzyme had been previously identified that converts 13-*cis*-retinoids to other retinoid isomers. Also, no biological function has ever been attributed to 13-*cis*-retinoids in eukaryotes. For these reasons, 13-*cis*-retinoids are thought to represent a metabolic ‘dead-end.’ However, 13-*cis*-retinoids do not accumulate in normal eyes, despite continued synthesis of 13-*cis*-ROL by Rpe65²⁹. This implies the existence of an enzyme that converts 13-*cis*-ROL into other isomers that can re-enter the visual cycle. Given the reversibility of DES1-catalyzed retinol isomerization, and the lower

free energy of all-*trans*-ROL versus 13-*cis*-ROL²⁸, DES1 may also function to eliminate 13-*cis*-ROL produced during chromophore biogenesis in RPE (Fig. 2a) and Müller cells (Fig. 6). Thus, DES1 may act as both a source and disposal mechanism for 13-*cis*-retinoids in ocular and extraocular tissues.

Within the neural retina, DES1 is expressed in Müller cells (Figs. 2a and b), the site of the proposed alternate visual cycle⁷⁻⁹. DES1 is also expressed in the RPE (Fig. 2b), where it may augment synthesis of 11-*cis*-ROL by Rpe65. Outside the eye, DES1 is expressed in multiple tissues including brain, liver, kidney and skin^{17,23}. In brain and skin, which contain large amounts of ceramide and other sphingolipids, DES1 may function primarily as a lipid desaturase. However, 9-*cis*-retinoic acid (9-*cis*-RA) is also present in multiple tissues where it binds with high affinity to both the retinoic-acid and retinoid-X receptors. DES1 is the only known source of 9-*cis*-retinoids in vertebrates. The 9-*cis*-ROL product of DES1 can be readily converted to 9-*cis*-RA. Thus, DES1 as isomerase-2 may play a part in non-visual processes such as cell growth, differentiation, apoptosis and malignant transformation by contributing to the synthesis of 9-*cis*-RA.

METHODS

Immunohistochemistry

Eye cups were prepared as previously described⁴⁷. Sections were reduced in 0.1 M NaBH₄ (Sigma) in pH 7.2 phosphate-buffered saline (PBS) (GIBCO, Invitrogen) followed by two five-min washes in PBS. Sections were permeabilized and blocked in blocking reagent (0.1% Triton X-100 and 1% BSA in PBS) for one hr. Primary antibodies were diluted 1:50 in blocking reagent and incubated overnight at 4°C. Rabbit anti-DES1 antisera specific to the mouse protein (Pacific Immunology) was visualized using a goat anti-rabbit AlexaFluor 488-conjugated secondary antibody (Invitrogen). CRALBP localization was achieved using a monoclonal anti-RLBP-1 (clone 1H7) antibody raised in mouse (Sigma) and visualized using a goat anti-mouse AlexaFluor 568-conjugated secondary antibody (Invitrogen). Slides were washed three times for 10 min in PBS. Secondary antibodies were diluted 1:100 in blocking reagent and incubated for one hr at room temp. Slides were washed thrice for 15 min and allowed to dry before the addition of ProLong Gold antifade reagent with DAPI mounting solution (Invitrogen). Slides were observed using an Olympus FluoView FV1000 confocal laser-scanning microscope under 40x and 60x oil-immersion objectives. Images were minimally processed (signal intensities were not manipulated) using Fiji software (Fig. 2).

Isomerase-2 Activity Assays

Isomerase-2 assays were performed using previously published procedures¹⁴. Reagents for these assays were from Sigma unless otherwise indicated. In brief, harvested cells were homogenized in glass-to-glass tissue grinders (Kontes) in ice-cold homogenization buffer (40 mM Tris pH 7.2 with 1 mM DL-dithiothreitol (DTT)). After homogenization, protein samples were kept on ice for immediate use. Aliquots of each homogenate were removed for protein determination (Micro BCA Protein Assay, Thermo Fisher). The enzyme assays were carried out in the dark at 37°C. Assay volumes were 500 µL and contained 0.2–0.5 mg

protein homogenate and 1–2% BSA. As indicated in the Supplementary Methods, assay conditions included 0–50 μM retinol substrate, 150–500 μM palmitoyl coenzyme A lithium salt (palm CoA), 500 μM reduced nicotinamide adenine dinucleotide phosphate (NADPH) and/or 0–500 μM oxidized NADP⁺. Reactions were carried out in pH 7.2 40 mM Tris buffer with 1 mM DTT. Assay reactions were placed in two mL amber glass vials (Agilent) and mixed continuously by inversion for two to 30 min at 37°C. All reactions were quenched by addition of 20 μL 5% SDS (Fisher), 50 μL 2M NaCl, and one mL ice-cold methanol, followed by vortexing.

Retinoid Analysis

All retinoid manipulations and extractions were performed under dim red light and analyzed by normal-phase HPLC as previously described¹³. Briefly, extracted retinoids were suspended in 200 μL of hexane (Sigma) and analyzed in an Agilent 1100 series chromatograph with a UV-visible photodiode array detector (spectral data range 318–365 nm). An Agilent Zorbax Rx-SIL column (4.6 \times 100 mm, 1.8 μm) with a gradient of 0.1–10% dioxane in hexane at a flow rate of 0.9 mL/min was used to resolve the sample. The identity of each eluted peak was established spectrally and by co-elution with authentic standards. Quantitation was performed by comparison of sample peak areas to calibration curves established with retinoid standards (Supplementary Fig. 1).

Co-immunoprecipitation of DES1 and CRALBP

Chicken retinas, or 293T cells transfected with a plasmid for chicken CRALBP, were incubated in Lysis/Wash buffer (25 mM Tris pH 7.4, 150 mM NaCl, 1 mM EDTA, 1% NP-40, 5% glycerol, and complete proteinase inhibitors - Roche) at 4°C on an orbital shaker for 30 min. The lysate was centrifuged at 13,000 \times g for 10 min in a 1.5 mL Eppendorf tube. The supernatant was collected and a small aliquot was removed for protein determination by the BCA assay. 150 μL of Dynabeads Protein A suspension (30 mg/mL) (Invitrogen) was added to a 1.5 mL Eppendorf tube. The tube was placed on a magnet and the supernatant removed. The Dynabeads were washed twice with 200 μL Lysis/Wash buffer. After removing the final Lysis/Wash buffer, 30 μg of affinity-purified rabbit polyclonal antiserum against chicken DES1, or rabbit polyclonal anti-RLBP1 (CRALBP) antiserum (Sigma-Aldrich) in 100 μL Lysis/Wash buffer was added to the tube containing the washed Dynabeads and incubated for 20 min with rotational mixing at room temperature. The supernatant was removed and the Dynabeads containing the immobilized antibodies were washed twice with Lysis/Wash buffer. Then, 200 μL of cell extract (10 mg/mL total-protein) was added to the Dynabeads-Ab complex and gently resuspended by pipetting. The tube was incubated at room temperature for 30 min. The supernatant was removed and the beads were washed three times with 200 μL of Lysis/Wash buffer by gently pipetting. The beads were resuspended in 100 μL Lysis/Wash buffer and transferred to a clean Eppendorf tube. The beads were washed with 200 μL of Conditioning buffer and resuspended in 20 μL of Elution buffer (200 mM glycine, pH 2.8). The suspension was incubated at room temperature for five min. The supernatant was collected for immunoblotting blotting after placing the tube on a magnet (Fig. 5a).

Immunoblot Analysis

Protein samples were harvested in PBS with protease inhibitor cocktail (Roche), homogenized, treated with 100 U DNase1 (Invitrogen) at 37°C for one hr, and re-homogenized in the presence of 1% SDS. Samples were spun briefly in a microfuge to pellet cell debris and the supernatants collected. Protein concentrations were determined using the BCA assay. Forty- μ g aliquots of each sample were loaded onto 12% Novex NuPAGE bis-tris gels (Invitrogen), run with Novex NuPAGE MOPS-SDS buffer (Invitrogen), and transferred to Immobilon-FL PVDF membranes (EMD-Millipore) using the Bio-Rad semi-dry transfer system. Blots were subsequently probed with the indicated antibodies in LI-COR Blocking Buffer with 0.5% donkey serum and 0.1% Tween 20 (Sigma). Secondary antibody staining and imaging were performed with LI-COR fluorescent-tagged antibodies and the LI-COR Odyssey infrared imaging system. Quantitative analyses were performed using LI-COR Odyssey analysis software, with protein normalized to alpha-tubulin (Sigma Aldrich antibody #T6199).

Chicken Müller Cell Primary Culture

Primary chicken Müller cell cultures were established according to published procedures⁹ with modifications to increase cell proliferation and restrict *trans*-differentiation. Freshly slaughtered chicken heads (non-scalded) were provided by Al Salam Polleria, Inc., Los Angeles, CA, and delivered on ice to our laboratory within two hr of slaughter. Cells were grown on 60 mm plates (CellBind, Corning) using minimum essential medium (MEM) containing 10% fetal bovine serum (FBS), 5 mg/mL glucose, 100 U/mL penicillin and 100 μ g/mL streptomycin at 37°C in 5% CO₂ (Invitrogen). The medium was changed 24 hr later and every 48 hr thereafter until cultured cells were confluent, usually within three to four weeks.

Intravitreal injection of Ad-DES1 and Ad-RFP

Recombinant adenoviruses (type-5) expressing DES1 (ad-DES1) or red fluorescent protein (ad-RFP) with the CMV promoter (Signagen) were injected intravitreally into four- to five-week-old *rpe65*^{-/-} eyes after anesthetizing with Ketamine (100 mg/kg, Phoenix Pharmaceutical) and Xylazine (10 mg/kg, Lloyd Laboratories). One- μ L aliquots containing 10⁷ ad-DES1 or ad-RFP viruses were injected into each eye using 34 g beveled needles and a trans-scleral approach. All experiments on mice were performed in accordance with protocol ARC #2001-061-33, approved by the Office of Animal Research Oversight at University of California, Los Angeles.

Electroretinography

ERGs were recorded as previously described⁴⁸. Briefly, after overnight dark-adaptation, ERGs were recorded from the corneal surface of both eyes using a gold-loop electrode referenced to a similar gold wire in the mouth. The mouse head was centered in an integrating sphere where light flashes were presented using a stereotaxic (Stoelting, USA) apparatus to ensure reproducibility between eyes tested. ERG responses from uninjected *rpe65*^{-/-} control mice showed no significant difference between eyes. Responses were amplified 10,000-fold (Grass P511 High Performance AC Amplifier), band-pass filtered

(0.1–300 Hz), and digitized using an I/O board (PCI-6221, National Instruments, Austin, TX) in a personal computer. ERG responses were recorded to white flashes of light modulated at 10 Hz. This flash presentation rate allowed extensive signal averaging and improved signal-to-noise ratios. A Fourier transformation was applied to the raw waveforms to extract responses at 10-Hz.

Statistical Analysis

All data values shown represent the mean for the number of replicates (n) indicated in each figure legend. Error bars represent standard errors of the mean (s.e.m.) or standard deviations (s.d.), as indicated. Student's t-test was used to determine the statistical significance between groups, where indicated.

Supplementary Material

Refer to Web version on PubMed Central for supplementary material.

Acknowledgments

We gratefully acknowledge Roxana Radu for her insightful suggestions throughout this project and valuable comments on the manuscript. We thank Jane Hu and Dean Bok for their assistance with the immunocytochemistry. We thank Mike Redmond for providing *rpe65*^{-/-} mice and Rosalie Crouch for her gift of 11-*cis*-RAL. This work was supported by a grant to G.H.T. from the National Eye Institute (R01-EY11713). G.H.T. is the Charles Kenneth Feldman Professor of Ophthalmology.

References

1. Crouch R, Purvin V, Nakanishi K, Ebrey T. Isorhodopsin II: artificial photosensitive pigment formed from 9,13-dicis retinal. Proceedings of the National Academy of Sciences of the United States of America. 1975; 72:1538–42. [PubMed: 1055424]
2. Jin M, Li S, Moghrabi WN, Sun H, Travis GH. Rpe65 is the retinoid isomerase in bovine retinal pigment epithelium. Cell. 2005; 122:449–59. [PubMed: 16096063]
3. Redmond TM, et al. Mutation of key residues of RPE65 abolishes its enzymatic role as isomerohydrolase in the visual cycle. Proc Natl Acad Sci U S A. 2005; 102:13658–63. [PubMed: 16150724]
4. Goldstein EB. Cone pigment regeneration in the isolated frog retina. Vision Res. 1970; 10:1065–8. [PubMed: 5492790]
5. Hood DC, Hock PA. Recovery of cone receptor activity in the frog's isolated retina. Vision Research. 1973; 13:1943–51. [PubMed: 4542882]
6. Jones GJ, Crouch RK, Wiggert B, Cornwall MC, Chader GJ. Retinoid requirements for recovery of sensitivity after visual-pigment bleaching in isolated photoreceptors. Proceedings of the National Academy of Sciences of the United States of America. 1989; 86:9606–10. [PubMed: 2594788]
7. Wang JS, Estevez ME, Cornwall MC, Kefalov VJ. Intra-retinal visual cycle required for rapid and complete cone dark adaptation. Nat Neurosci. 2009; 12:295–302. [PubMed: 19182795]
8. Wang JS, Kefalov VJ. An alternative pathway mediates the mouse and human cone visual cycle. Curr Biol. 2009; 19:1665–9. [PubMed: 19781940]
9. Das SR, Bhardwaj N, Kjeldbye H, Gouras P. Muller cells of chicken retina synthesize 11-*cis*-retinol. Biochemical Journal. 1992; 285:907–13. [PubMed: 1497628]
10. Bunt-Milam AH, Saari JC. Immunocytochemical localization of two retinoid-binding proteins in vertebrate retina. Journal of Cell Biology. 1983; 97:703–12. [PubMed: 6350319]
11. Eisenfeld AJ, Bunt-Milam AH, Saari JC. Localization of retinoid-binding proteins in developing rat retina. Exp Eye Res. 1985; 41:299–304. [PubMed: 3905423]

12. Wu BX, et al. Identification of RDH10, an All-trans Retinol Dehydrogenase, in Retinal Muller Cells. *Invest Ophthalmol Vis Sci*. 2004; 45:3857–62. [PubMed: 15505029]
13. Mata NL, Radu RA, Clemmons R, Travis GH. Isomerization and oxidation of vitamin a in cone-dominant retinas. A novel pathway for visual-pigment regeneration in daylight. *Neuron*. 2002; 36:69–80. [PubMed: 12367507]
14. Mata NL, Ruiz A, Radu RA, Bui TV, Travis GH. Chicken retinas contain a retinoid isomerase activity that catalyzes the direct conversion of all-trans-retinol to 11-cis-retinol. *Biochemistry*. 2005; 44:11715–21. [PubMed: 16128572]
15. Muniz A, et al. Evidence for two retinoid cycles in the cone-dominated chicken eye. *Biochemistry*. 2009; 48:6854–63. [PubMed: 19492794]
16. Moiseyev G, Chen Y, Takahashi Y, Wu BX, Ma JX. RPE65 is the isomerohydrolase in the retinoid visual cycle. *Proc Natl Acad Sci U S A*. 2005; 102:12413–8. [PubMed: 16116091]
17. Cadena DL, Kurten RC, Gill GN. The product of the MLD gene is a member of the membrane fatty acid desaturase family: overexpression of MLD inhibits EGF receptor biosynthesis. *Biochemistry*. 1997; 36:6960–7. [PubMed: 9188692]
18. Savile CK, Fabrias G, Buist PH. Dihydroceramide delta4 Desaturase Initiates Substrate Oxidation at C-4. *J Am Chem Soc*. 2001; 123:4382–4385. [PubMed: 11457221]
19. Shanklin J, Whittle E, Fox BG. Eight histidine residues are catalytically essential in a membrane-associated iron enzyme, stearoyl-CoA desaturase, and are conserved in alkane hydroxylase and xylene monooxygenase. *Biochemistry*. 1994; 33:12787–94. [PubMed: 7947684]
20. Michel C, et al. Characterization of ceramide synthesis. A dihydroceramide desaturase introduces the 4,5-trans-double bond of sphingosine at the level of dihydroceramide. *The Journal of biological chemistry*. 1997; 272:22432–7. [PubMed: 9312549]
21. Rioux V, Pedrono F, Legrand P. Regulation of mammalian desaturases by myristic acid: N-terminal myristoylation and other modulations. *Biochimica et biophysica acta*. 2011; 1811:1–8. [PubMed: 20920594]
22. Beauchamp E, et al. N-Myristoylation targets dihydroceramide Delta4-desaturase 1 to mitochondria: partial involvement in the apoptotic effect of myristic acid. *Biochimie*. 2009; 91:1411–9. [PubMed: 19647031]
23. Causeret C, Geeraert L, Van der Hoeven G, Mannaerts GP, Van Veldhoven PP. Further characterization of rat dihydroceramide desaturase: tissue distribution, subcellular localization, and substrate specificity. *Lipids*. 2000; 35:1117–25. [PubMed: 11104018]
24. Beauchamp E, et al. Myristic acid increases the activity of dihydroceramide Delta4-desaturase 1 through its N-terminal myristoylation. *Biochimie*. 2007; 89:1553–61. [PubMed: 17716801]
25. Triola G, Fabrias G, Casas J, Llebaria A. Synthesis of cyclopropene analogues of ceramide and their effect on dihydroceramide desaturase. *The Journal of organic chemistry*. 2003; 68:9924–32. [PubMed: 14682684]
26. Rahmaniyan M, Curley RW Jr, Obeid LM, Hannun YA, Kravets JM. Identification of Dihydroceramide Desaturase as a Direct in vitro target for Fenretinide. *The Journal of biological chemistry*. 2011
27. Rando RR, Chang A. Studies on the catalyzed interconversion of vitamin A derivatives. *J Am Chem Soc*. 1983; 105:2879–2882.
28. Rando RR. Molecular mechanisms in visual pigment regeneration. *Photochemistry & Photobiology*. 1992; 56:1145–56. [PubMed: 1492129]
29. Redmond TM, Poliakov E, Kuo S, Chander P, Gentleman S. RPE65, visual cycle retinol isomerase, is not inherently 11-cis-specific: support for a carbocation mechanism of retinol isomerization. *The Journal of biological chemistry*. 2010; 285:1919–27. [PubMed: 19920137]
30. Trevino SG, Villazana-Espinoza ET, Muniz A, Tsun AT. Retinoid cycles in the cone-dominated chicken retina. *J Exp Biol*. 2005; 208:4151–7. [PubMed: 16244173]
31. Kefalov VJ, et al. Breaking the covalent bond--a pigment property that contributes to desensitization in cones. *Neuron*. 2005; 46:879–90. [PubMed: 15953417]
32. Redmond TM, et al. Rpe65 is necessary for production of 11-cis-vitamin A in the retinal visual cycle. *Nature Genetics*. 1998; 20:344–51. [PubMed: 9843205]

33. Znoiko SL, et al. Downregulation of cone-specific gene expression and degeneration of cone photoreceptors in the Rpe65^{-/-} mouse at early ages. *Investigative ophthalmology & visual science*. 2005; 46:1473–9. [PubMed: 15790918]
34. Di Polo A, Aigner LJ, Dunn RJ, Bray GM, Aguayo AJ. Prolonged delivery of brain-derived neurotrophic factor by adenovirus-infected Muller cells temporarily rescues injured retinal ganglion cells. *Proceedings of the National Academy of Sciences of the United States of America*. 1998; 95:3978–83. [PubMed: 9520478]
35. Saari JC, Bredberg DL. Photochemistry and stereoselectivity of cellular retinaldehyde-binding protein from bovine retina. *J Biol Chem*. 1987; 262:7618–22. [PubMed: 3584132]
36. Golovleva I, et al. Disease-causing mutations in the cellular retinaldehyde binding protein tighten and abolish ligand interactions. *J Biol Chem*. 2003; 278:12397–402. [PubMed: 12536144]
37. Saari JC, Nawrot M, Stenkamp RE, Teller DC, Garwin GG. Release of 11-cis-retinal from cellular retinaldehyde-binding protein by acidic lipids. *Mol Vis*. 2009; 15:844–54. [PubMed: 19390642]
38. Hubbard R. The thermal stability of rhodopsin and opsin. *J Gen Physiol*. 1958; 42:259–80. [PubMed: 13587911]
39. Meyer DB, May HC Jr. The topographical distribution of rods and cones in the adult chicken retina. *Experimental Eye Research*. 1973; 17:347–55. [PubMed: 4765257]
40. Carter-Dawson LD, LaVail MM. Rods and cones in the mouse retina. I. Structural analysis using light and electron microscopy. *J Comp Neurol*. 1979; 188:245–62. [PubMed: 500858]
41. Rohrer B, et al. Correlation of regenerable opsin with rod ERG signal in Rpe65^{-/-} mice during development and aging. *Investigative ophthalmology & visual science*. 2003; 44:310–5. [PubMed: 12506090]
42. Caruso RC, et al. Retinal disease in Rpe65-deficient mice: comparison to human leber congenital amaurosis due to RPE65 mutations. *Investigative ophthalmology & visual science*. 2010; 51:5304–13. [PubMed: 20484585]
43. Fan J, Rohrer B, Moiseyev G, Ma JX, Crouch RK. Isorhodopsin rather than rhodopsin mediates rod function in RPE65 knock-out mice. *Proc Natl Acad Sci U S A*. 2003; 100:13662–7. [PubMed: 14578454]
44. Farjo KM, Moiseyev G, Takahashi Y, Crouch RK, Ma JX. The 11-cis-retinol dehydrogenase activity of RDH10 and its interaction with visual cycle proteins. *Investigative ophthalmology & visual science*. 2009; 50:5089–97. [PubMed: 19458327]
45. Baylor DA, Nunn BJ, Schnapf JL. The photocurrent, noise and spectral sensitivity of rods of the monkey *Macaca fascicularis*. *J Physiol*. 1984; 357:575–607. [PubMed: 6512705]
46. Hsu SC, Molday RS. Glucose metabolism in photoreceptor outer segments. Its role in phototransduction and in NADPH-requiring reactions. *The Journal of biological chemistry*. 1994; 269:17954–9. [PubMed: 8027053]
47. Radu RA, et al. Reductions in serum vitamin a arrest accumulation of toxic retinal fluorophores: a potential therapy for treatment of lipofuscin-based retinal diseases. *Invest Ophthalmol Vis Sci*. 2005; 46:4393–401. [PubMed: 16303925]
48. Nusinowitz S, Ridder WH 3rd, Ramirez J. Temporal response properties of the primary and secondary rod-signaling pathways in normal and Gnat2 mutant mice. *Experimental eye research*. 2007; 84:1104–14. [PubMed: 17408617]

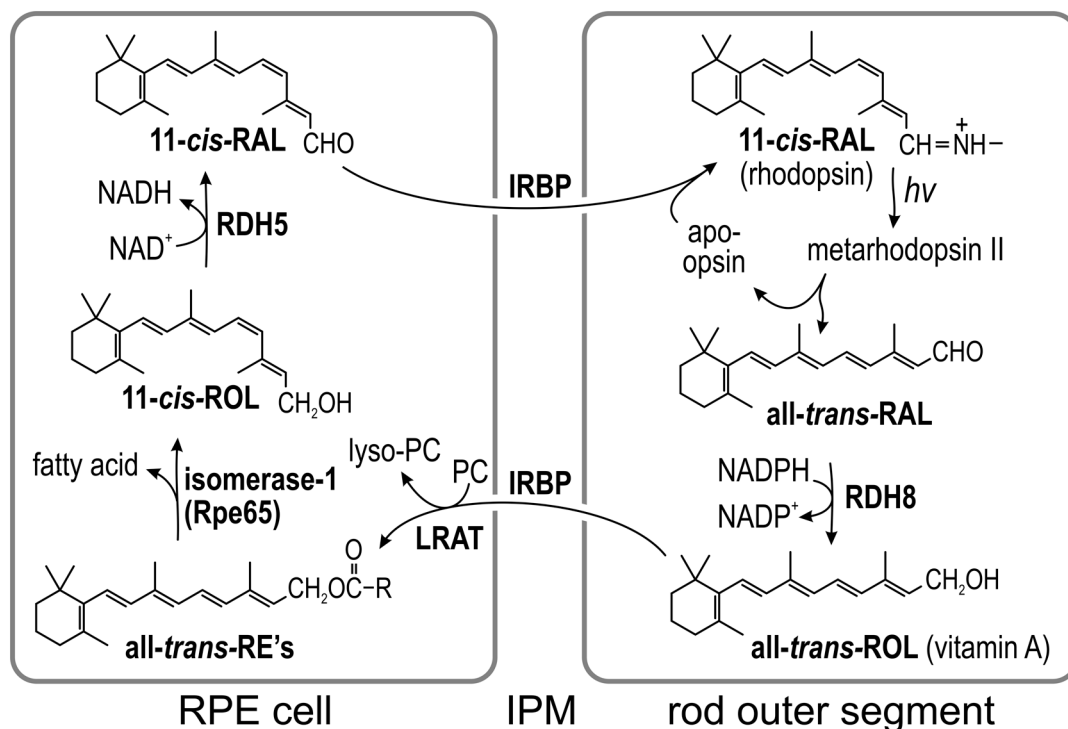


Figure 1. Visual cycle in RPE cells

The light sensitive protein in rod photoreceptors is rhodopsin, located within the membranous outer-segment. Rhodopsin contains the visual chromophore, 11-*cis*-retinaldehyde (11-*cis*-RAL). Absorption of a photon ($h\nu$) induces 11-*cis* to all-*trans* isomerization of the chromophore, converting rhodopsin into active metarhodopsin II. Metarhodopsin II decays to yield apo-opsin and free all-*trans*-retinaldehyde (all-*trans*-RAL). The all-*trans*-RAL is reduced by NADPH-dependent retinol dehydrogenase type-8 (RDH8) to all-*trans*-retinol (all-*trans*-ROL). The all-*trans*-ROL is released by the outer segment into the IPM where it binds IRBP. The all-*trans*-ROL is taken up by RPE apical processes where it is esterified to a fatty acid by lecithin:retinol acyl transferase (LRAT) utilizing phosphatidylcholine (PC) as an acyl-donor. The resulting all-*trans*-retinyl esters (all-*trans*-RE's) are the substrate for isomerase-1 (Rpe65), which catalyzes both hydrolysis of the ester and isomerization of all-*trans*-ROL to 11-*cis*-retinol (11-*cis*-ROL). The final catalytic step in the visual cycle is oxidation of 11-*cis*-ROL to 11-*cis*-RAL by retinol dehydrogenase type-5 (RDH5). 11-*cis*-RAL is released by the RPE into the IPM where it binds IRBP and is subsequently taken up by a rod outer segment where it recombines with an apo-opsin to form a new rhodopsin pigment molecule.

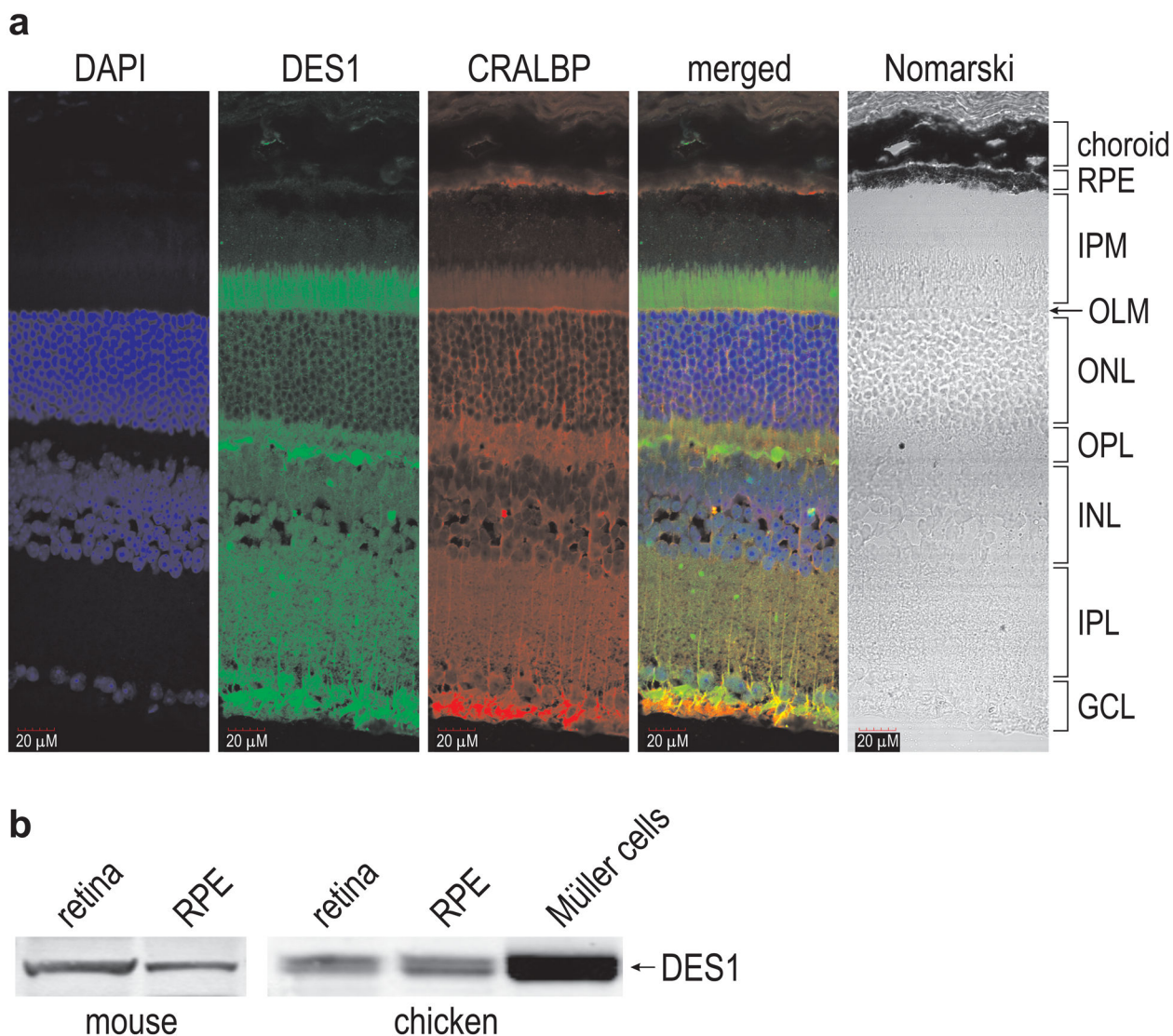


Figure 2. Immunohistochemical and immunoblot analysis showing DES1 expression in the retina and RPE

(a) Sections from a six-month-old 129/Sv mouse retina were reacted with antibodies against mouse DES1 (green) or CRALBP (red). Nuclei were counter-stained with DAPI (blue). The merged image shows overlapping expression of DES1 and CRALBP (yellow). Morphologic features of the retina are shown to the right of the Nomarski image. RPE, retinal pigment epithelium; IPM, interphotoreceptor matrix; OLM, outer limiting membrane; ONL, outer nuclear layer; OPL, outer plexiform layer; INL, inner nuclear layer; IPL, inner plexiform layer; GCL, ganglion cell layer. Note that DES1- and CRALBP-containing apical processes of Müller cells extend into the IPM, which also contains photoreceptor outer segments and the apical processes of RPE cells. The Müller-cell endfeet contact the vitreous within the GCL. Scale bar shows 20 μm . (b) Immunoblots showing DES1 in mouse retina and RPE (left), and chicken retina, RPE and primary cultured Müller cells (right).

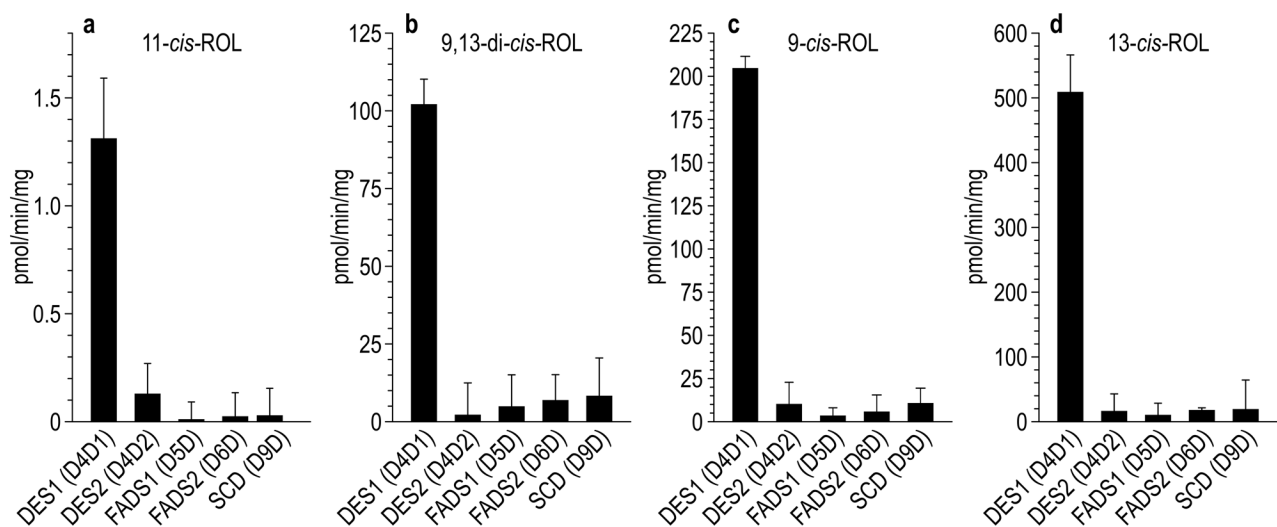


Figure 3. Isomerase-2 activities of human membrane desaturases

DES1, DES2, FADS1, FADS2 and SCD were expressed in 293T cells. Cell homogenates were assayed for synthesis of 11-*cis*-ROL (a), 9,13-di-*cis*-ROL (b), 9-*cis*-ROL (c) and 13-*cis*-ROL (d), using all-*trans*-ROL as substrate. Activities are expressed as pmoles per minute per mg-total protein (n=3; s.e.m.).

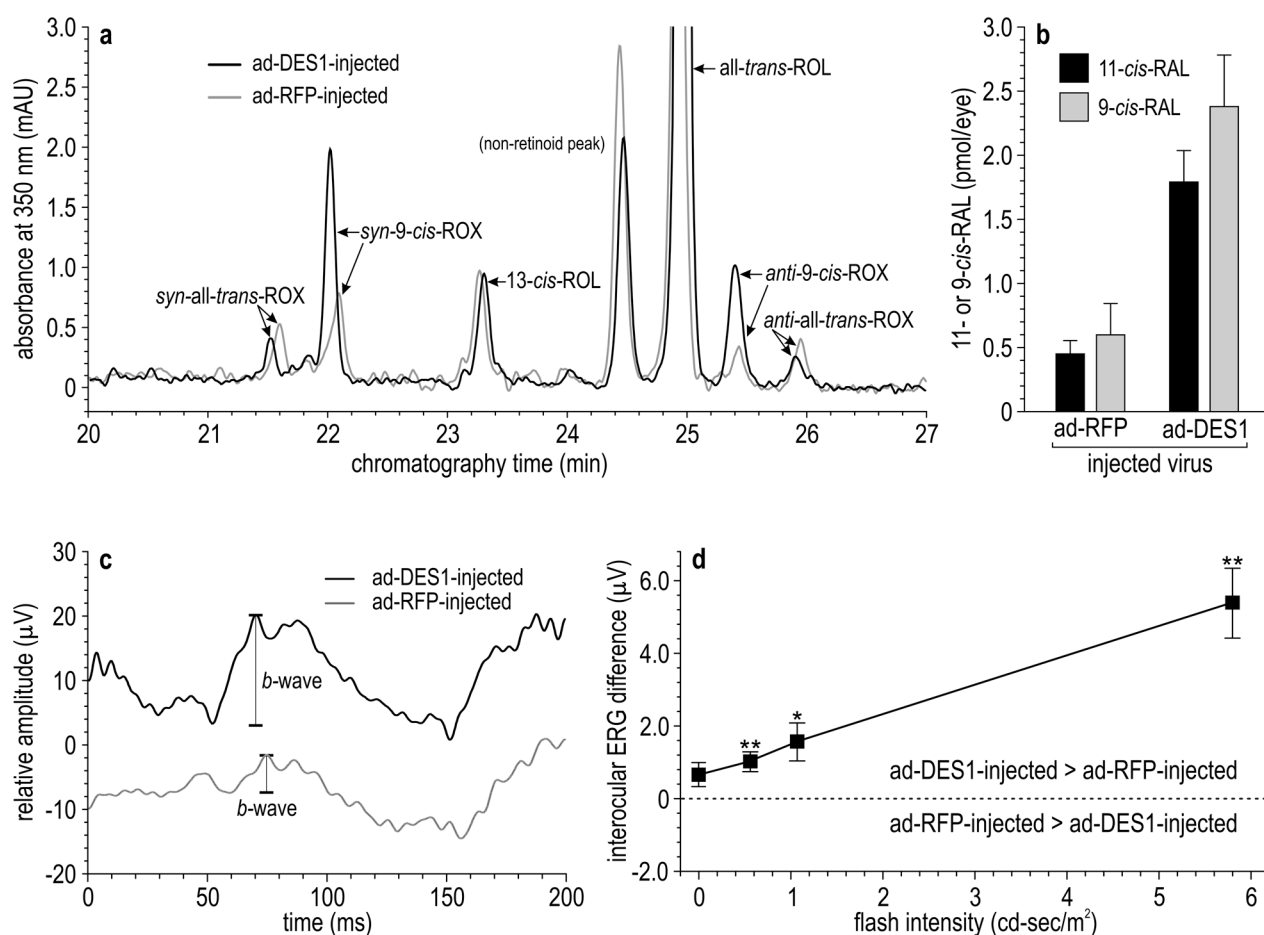


Figure 4. Levels of visual chromophore and ERG amplitudes in *rpe65*^{-/-} mice after intravitreal injection of ad-DES1 or ad-RFP

(a) Normal-phase chromatogram showing elution of retinaldehyde oximes (ROX) and retinols in extracts of *rpe65*^{-/-} retinas following intravitreal injection of ad-DES1 (red tracing) or ad-RFP (gray tracing). Peaks containing *syn*- and *anti*- oximes for all-*trans*-RAL and 9-*cis*-RAL are labeled. Note the elevated 9-*cis*-RAL (*syn*- and *anti*-9-*cis*-ROX). 11-*cis*-RAL oximes were undetectable in these mice that received no supplemental all-*trans*-ROL. (b) Levels of 11-*cis*-RAL and 9-*cis*-RAL in extracts of *rpe65*^{-/-} retinas following intravitreal injection of ad-DES1 (black bars) or ad-RFP (gray bars). Mice in this experiment received 5.0 nmoles of intravitreal all-*trans*-ROL supplementation. Background levels of 9-*cis*-RAL and 11-*cis*-RAL in ad-RFP-injected *rpe65*^{-/-} eyes were from thermal isomerization and oxidation of the added all-*trans*-ROL substrate (n=9; s.e.m.). (c) Representative dark-adapted ERGs recorded to the brightest flash (5.791 cd-s/m²) modulated at 10 Hz in *rpe65*^{-/-} mice after intravitreal injection of ad-DES1 (black tracing) or ad-RFP (gray tracing). Shown are the first 200 msec of the responses. Tracings are vertically displaced for clarity (d) Interocular differences in Fourier-derived ERG responses between eyes injected with ad-DES1 versus ad-RFP. Positive interocular amplitude differences (values > 0) indicate that the eye receiving the ad-DES1 injection performed better than the ad-RFP eye (n=9; s.d.; * p<0.05, ** p<0.01).

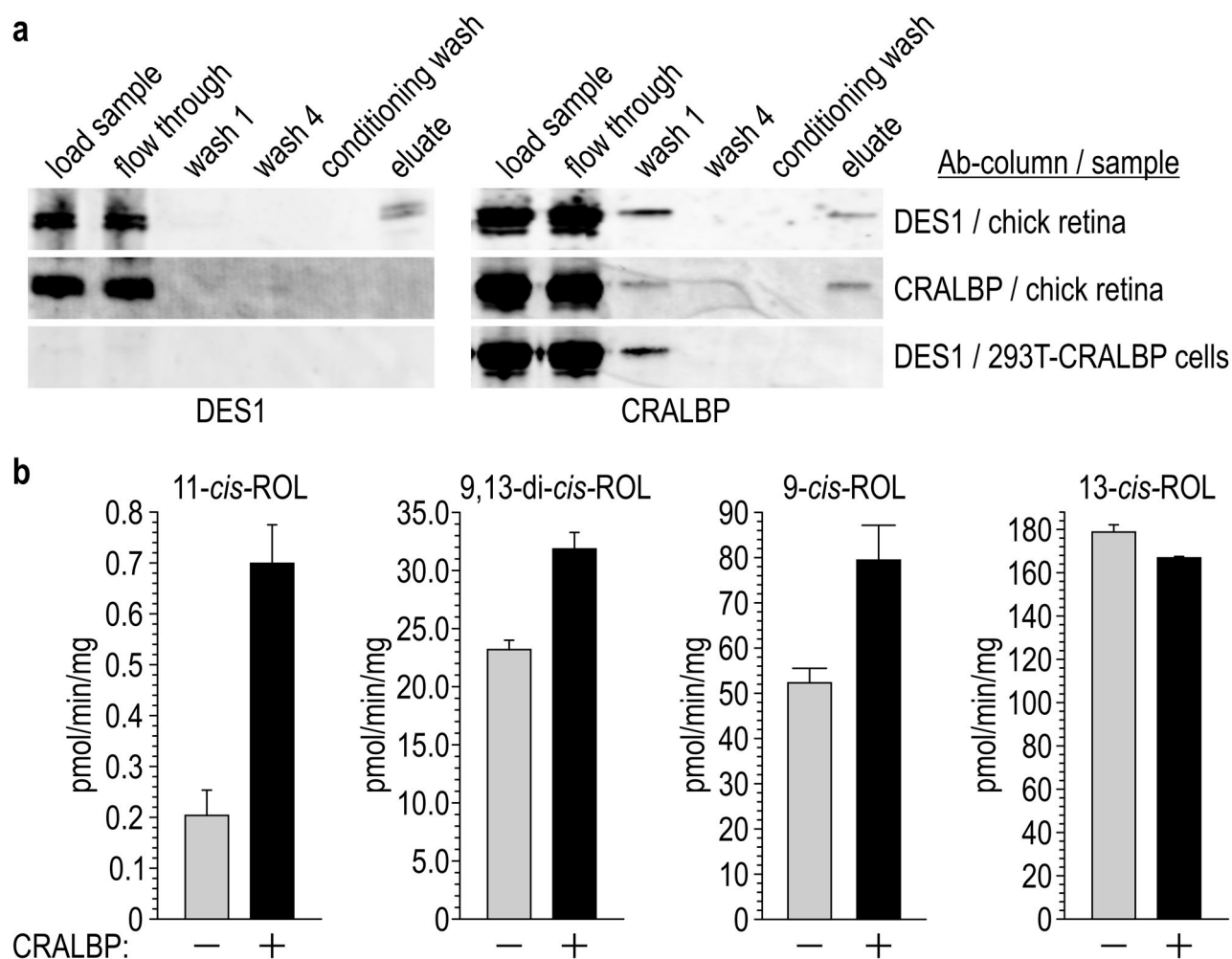


Figure 5. Co-immunoprecipitation of CRALBP with DES1 and effects of CRALBP on isomerase-2 activity

(a) Immunoblots of protein samples detected with antibodies against chicken DES1 or CRALBP. Samples include the starting homogenates (load sample); unbound samples after incubation with immobilized DES1 or CRALBP antibody (flow through); unbound samples after the first (wash 1) or final (wash 4) wash of the column with wash/lysis buffer; unbound samples after washing with Conditioning buffer (conditioning buffer); and eluted proteins after washing with elution buffer (eluate). Homogenates were from chicken retinas (first and second rows of blots) or 293T-cells expressing CRALBP (third row of blots). (b) Isomerase-2 activities of 293T-D cell homogenates that stably express DES1 minus or plus transient transfection with CRALBP. Figures show synthesis rates of 11-*cis*-ROL, 9,13-di-*cis*-ROL, 9-*cis*-ROL, and 13-*cis*-ROL expressed as specific activities (pmol/min/mg-total protein) (n=3; s.e.m.).

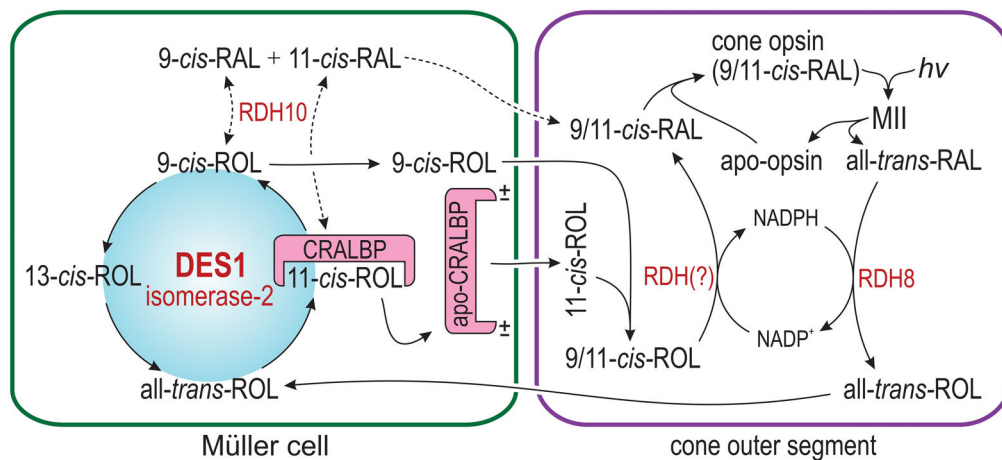


Figure 6. Proposed alternate visual cycle in Müller cells

Cone opsins use 11-*cis*-RAL or 9-*cis*-RAL (9/11-*cis*-RAL) as visual chromophore. Absorption of a photon by a cone opsin isomerizes the 9/11-*cis*-RAL to all-*trans*-RAL, as in rods. After reduction by RDH8 in the cone OS, the all-*trans*-ROL is released into the IPM and taken up by a Müller cell. Here, the all-*trans*-ROL is isomerized by DES1 to 11-*cis*-ROL, which is bound to CRALBP, and to 9-*cis*-ROL and 13-*cis*-ROL, which are not. CRALBP interacts with DES1 and protects 11-*cis*-ROL from further isomerization. Interaction with negatively charged phospholipids causes holo-CRALBP to release its 11-*cis*-ROL ligand into the IPM, where it binds IRBP and subsequently is taken up by a cone outer segment. In contrast, the 9-*cis*-ROL diffuses directly into the IPM without binding to CRALBP. In the cone OS, 9-*cis*- and 11-*cis*-ROL (9/11-*cis*-ROL) are oxidized by an unknown NADP⁺-dependent retinol dehydrogenase to 9/11-*cis*-RAL, which combine with apo-opsin to form a new opsin pigment. Simultaneous reduction of all-*trans*-RAL and oxidation of 9/11-*cis*-ROL in the cone OS provides a self-renewing supply of NADPH/NADP⁺ cofactors. Müller cells express RDH10, which non-specifically oxidizes retinol isomers to their cognate aldehydes. The resulting 9/11-*cis*-RAL may be utilized as chromophore by rod or cone apo-opsins. This is the likely source of iso-rhodopsin in *rpe65*^{-/-} retinas.

Table 1

Endogenous Retinoids in Mouse and Chicken Retinas (pmol/mg-protein)

	11-cis-	9,13-di-cis-	9-cis-	13-cis-	all-trans-	
mouse	11.7 ± 0.7	n.d.	2.01 ± 0.62	1.82 ± 0.14	7.40 ± 1.10	retinols
chicken	120 ± 11	29.8 ± 2.5	20.3 ± 0.9	46.5 ± 3.2	259 ± 20	
mouse	689 ± 37	n.d.	1.52 ± 0.17	3.66 ± 0.20	36.0 ± 1.7	retinaldehydes
chicken	590 ± 40	n.d.	38.6 ± 4.4	47.4 ± 6.7	215 ± 11	
mouse	n.d.	n.d.	n.d.	n.d.	n.d.	retinyl esters
chicken	255 ± 3	n.d.	27.3 ± 4.1	49.3 ± 5.9	41.3 ± 1.5	